Superoxide anion and proteasomal dysfunction contributes to curcumin-induced paraptosis of malignant breast cancer cells

Mi Jin Yoon, Eun Hee Kim, Jun Hee Lim, Taeg Kyu Kwon, Kyeong Sook Choi

PII: S0891-5849(09)00787-4
DOI: doi:10.1016/j.freeradbiomed.2009.12.016
Reference: FRB 10051

To appear in: *Free Radical Biology and Medicine*

Received date: 18 July 2009
Revised date: 7 November 2009
Accepted date: 17 December 2009

Please cite this article as: Mi Jin Yoon, Eun Hee Kim, Jun Hee Lim, Taeg Kyu Kwon, Kyeong Sook Choi, Superoxide anion and proteasomal dysfunction contributes to curcumin-induced paraptosis of malignant breast cancer cells, *Free Radical Biology and Medicine* (2009), doi:10.1016/j.freeradbiomed.2009.12.016

Superoxide anion and proteasomal dysfunction contributes to curcumin-induced paraptosis of malignant breast cancer cells

Mi Jin Yoon [a], Eun Hee Kim [a], Jun Hee Lim [b], Taeg Kyu Kwon [b], Kyeong Sook Choi [a,*]

[a] *Department of Molecular Science & Technology, Institute for Medical Sciences, Ajou University School of Medicine, Suwon, Korea*

[b] *Department of Immunology, Keimyung University School of Medicine, Taegu, Korea*

[*] Corresponding author: Kyeong Sook Choi

Department of Molecular Science & Technology

Institute for Medical Sciences

Ajou University School of Medicine

Suwon, Korea

Tel) 82-31-219-4552

Fax) 82-31-219-4530

E-mail) kschoi@ajou.ac.kr

Running title: Curcumin-induced paraptosis

Abstract

Curcumin is considered a pharmacologically safe agent that may be useful in cancer chemoprevention and therapy. Here, we show for the first time that curcumin effectively induces paraptosis in malignant breast cancer cell lines, including MDA-MB-435S, MDA-MB-231 and Hs578T cells, by promoting vacuolation that results from swelling and fusion of mitochondria and/or the endoplasmic reticulum (ER). Inhibition of protein synthesis by cycloheximide blocked curcumin-induced vacuolation and subsequent cell death, indicating that protein synthesis is required for this process. The levels of AIP-1/Alix protein, a known inhibitor protein of paraptosis, were progressively downregulated in curcumin-treated malignant breast cancer cells, and AIP-1/Alix overexpression attenuated curcumin-induced death in these cells. ERK2 and JNK activation were positively associated with curcumin-induced cell death. Mitochondrial superoxide was shown to act as a critical early signal in curcumin-induced paraptosis, whereas proteasomal dysfunction was mainly responsible for the paraptotic changes associated with ER dilation. Notably, curcumin-induced paraptotic events were not observed in normal breast cells, including mammary epithelial cells and MCF-10A cells. Taken together, our findings on curcumin-induced paraptosis may provide novel insights into the mechanisms underlying the selective anti-cancer effects of curcumin against malignant cancer cells.

Keywords: Curcumin, Paraptosis, Superoxide anion, Proteasome, Breast cancer cells

Introduction

Curcumin (diferuloylmethane), a major active component of turmeric (*Curcuma longa*), has long been used as a popular dietary spice and herbal medicine in the Orient [1]. Curcumin acts on a variety of molecular targets associated with cancer development, and preclinical data have shown that it can inhibit tumor formation in animal models of carcinogenesis [2]. Clinical trials have revealed that curcumin may produce antitumor effects in individuals with precancerous lesions or those who are at a high risk for developing cancer [3]. Furthermore, curcumin has demonstrated selective killing of various cancer cell types, while sparing normal cells [3-5]. Such observations suggest that curcumin is a pharmacologically safe agent that may be used not only in cancer chemoprevention, but also in cancer therapy, either as a primary therapeutic agent or as an adjuvant to traditional chemotherapy. Although much of the research into the cancer-killing effects of curcumin has focused on its ability to induce apoptosis [2,3,6,7], curcumin has also been reported to induces non-apoptotic cell death through mitotic catastrophe [8,9] or autophagic cell death [10] in several types of cancer cells.

Recently, a new type of non-apoptotic cell death, termed paraptosis (from *para* = next to or related to, and *apoptosis*) [11], has been reported to be induced by insulin-like growth factor 1 receptor, epidermal growth factor, and TAJ/TROY, a member of the tumor necrosis factor receptor superfamily [12-14]. Paraptosis is characterized by a process of vacuolation that begins with physical enlargement of mitochondria and the ER [11,14,15]. This form of cell death does not involve the apoptotic characteristics of pyknosis, DNA fragmentation or caspase activation [11]. Paraptosis is known to require new protein synthesis [11], and recent reports have identified AIP-1/Alix as an inhibitor of paraptosis [12,16]. However, the mechanisms underlying paraptosis, in particular the

signals responsible for triggering mitochondrial and ER dilation, have not yet been fully determined.

Here we show that curcumin is preferentially cytotoxic to malignant breast cancer cells compared with normal breast cells, and demonstrate that cell death is due to induction of paraptosis, not apoptosis or autophagy. We further show that superoxide anion and proteasomal dysfunction contribute to the paraptotic changes seen in mitochondria and the ER.

Materials and Methods

Chemicals and antibodies

We used the following chemicals: 3-methyladenine (3-MA), bafilomycin A1, cycloheximide (CHX), lactacystin, MG132, N-acetylcysteine (NAC), reduced glutathione (GSH), polyethylene glycol (PEG)-catalase (Sigma Chemical Corp); MitoTracker-Red, MitoTracker-Green, ER Tracker-Red, calcein acetoxymethyl ester (calcein-AM), ethidium homodimer (EthD-1), 5-6-carboxy-2',7'-dichlorofluorescein diacetate (H_2DCF-DA), MitoSOX Red (Molecular Probe); z-VAD-fmk (R&D systems); MnTBAP (Mn(III)tetralis (benxoic acid porphyrin), SB203580, U0126, SP600125 (Calbiochem); N-acetyl-leucyl-leucyl-norleucinal (ALLN) (BioMol Research Laboratories; Recombinant TRAIL (KOMA). We used antibodies against β-actin, Flag-M2 (Sigma); caspase-3, caspase-4, caspase-7, XIAP, KDEL, survivin (Stressgen); Bcl-2, Bcl-xL, ubiquitin, ATG6, CHOP/GADD153 (Santa Cruz); PARP (Epitomics Inc.);

ATG7 (Prosci Inc.); phospho-ERK1/2, ERK1/2, phospho-p38, p38, phospho-JNK, JNK, phopho-eIF2α, eIF2α, AIP-1/Alix (Cell Signaling); hemagglutinin (HA) (Covance); rabbit IgG HRP, mouse IgG HRP (Zymed).

Cell culture and curcumin treatment

MDA-MB-231, MDA-MB-435S, and Hs578T were from American Type Culture Collection (ATCC), and cultured in DMEM supplemented with 10% fetal bovine serum and antibiotics (Life Technologies). MCF-10A (from ATCC) was cultured in serum-free Mammary Epithelial Growth Medium (MEGM, Clonetics Corp.) supplemented with 100 ng/ml cholera toxin. Normal human mammary epithelial cells (from Clonetics Corp.) were maintained in MEGM supplemented with bovine pituitary extract, insulin, human epidermal growth factor, hydrocortisone, and antibiotics. Cell culture passage number less than five was used in the present study. Curcumin (> 94% purity, Sigma) was dissolved in dimethyl sulfoxide (DMSO) at a concentration of 40 mM and stored in a dark colored bottle at -20°C. This stock solution was diluted to the required concentration when need.

Measurement of cellular viability

Cell viability was assessed by double labeling of cells with 2 μM calcein-AM and 4 μM EthD-1. The calcein-positive live cells and EthD-1-positive dead cells were visualized using fluorescence microscope (Axiovert 200M, Zeiss) and counted.

Western blotting

Cells were washed in PBS an lysed in boiling sodium dodecyl sulfate/polyacrylamide gel electrophoresis (SDS-PAGE) sample buffer (62.5 mM Tris [pH6.8], 1% SDS, 10% glycerol, and 5% β-mercaptoethanol). The lysates were boiled for 5 min, separated by SDS-PAGE, and transfected to an Immobilon membrane (Millipore). After blocking nonspecific binding sites for 1 h by 5% skim milk, membranes were incubated for 2 h with specific Abs. Membranes were then washed three times with TBST and incubated further for 1 h with horseradish peroxidase-conjugated anti-rabbit, mouse, or goat antibody. Visualization of protein bands was accomplished using ECL (Amersham Life Science). The respective protein band intensity was quantified by densitometric analysis using the NIH ImageJ program. The representative results from at least three independent experiments are shown.

Establishment of the stable cell lines expressing GFP-LC3 and the fluorescence specifically in mitochondria or endoplasmic reticulum

MDA-MB-435S cells were transfected with the plasmid encoding GFP-LC3 [17], the pEYFP-Mito, or pEYFP-ER vector (Clontech Laboratories), and the respective stable cell lines were selected with changes of medium containing 500 μg/ml G418.

Measurement of ROS and mitochondrial superoxide production

To measure ROS or mitochondrial superoxide production, cells were loaded with 10

μM H_2DCF-DA for 30 min in the dark, or loaded with 2.5 μM MitoSOX Red for 20 min in the dark. After washing with PBS or HBSS with Ca^{2+} and Mg^{2+}, cells were further processed for flow cytometry.

Establishment of the stable breast cancer cells overexpressing MnSOD or catalase

From the plasmids encoding hemagglutinin (HA)-tagged MnSOD or catalase [18], the respective antioxidant cDNAs were PCR amplified, and subcloned into MFG retroviral vector by replacing the GFP sequence of MFG.GFP.IRES.puro [19]. The respective retroviral plasmids were introduced into the 293gpg retrovirus packaging cell line by transfection with Lipofectamine. After 72 h, the supernatants were harvested and used for retroviral infection. Control cells were transfected with MFG alone. Stable cell lines overexpressing MnSOD or catalase were selected with changes of fresh media containing 4 μg/ml puromycin. The expressions of the respective antioxidant protein in the stable cell lines were analyzed by Western blotting using anti-HA antibody.

Small interfering RNAs

The small interfering RNA (siRNA) duplexes used in this study were purchased from Invitrogen and have the following sequences: ATG6 (NCBI accession No. NM-003799, CAGUUUGGCACAAUCAA UAACUUCA); ATG7 (NM-006395, CAGAAGGAGUCACAGCUCUUCCUUA); ERK2 (HUMERK2A, AAGAGGAUUGAAGUAGAACAGTT); ERK1 (Invitrogen Cat. No. 12935-200, UUAGAGAGCAUCUCAGCCAGAAUGC). After annealing of the pairs of siRNA

oligos, cells in 24-well plates were transfected with 40 nM siRNA oligonucleotides using Lipofectamine 2000 regent (Invitrogen) according to the manufacturer's instructions.

Transmission electron microscopy

Cells were prefixed in Karnovsky's solution [1% paraformaldehyde, 2% glutaraldehyde, 2 mM calcium chloride, 0.1 M cacodylate buffer (pH 7.4)] for 2 h and washed with cacodylate buffer. Post-fixing was carried out in 1% osmium tetroxide and 1.5% potassium ferrocyanide for 1 h. After dehydration with 50% to 100% alcohol, the cells were embedded in Poly/Bed 812 resin (Pelco) and polymerized and observed under electron microscope (EM 902A, Zeiss).

Construction of the expression vector encoding AIP-1/Alix

The human AIP-1/Alix cDNA was amplified by PCR using primers designed to incorporate a 5' Flag epitope. The PCR product was subcloned into the pcDNA3 expression vector (Invitrogen). The fidelity of the PCR and cloning procedures was verified by nucleotide sequencing.

Statistical analysis

All data were presented as mean ± S.D. (standard deviation) from at least three separate experiments. The statistical significance was assessed using ANOVA with

Bonferroni or repeated measures ANOVA followed by Greenhouse-Geisser adjustment. *P* values less than 0.05 were considered statistically significant.

Results

The selective cytotoxic effects of curcumin on malignant breast cancer cells are not associated with apoptosis or autophagy

An examination of the effects of curcumin on the viability of various cancer cells (MDA-MB-231, MDA-MB-435S and Hs578T) and normal cells of breast origin (human mammary epithelial cells [HMECs] and MCF-10A) revealed that curcumin was much more cytotoxic to malignant breast cancer cells than normal cells (Fig. 1A). We next investigated whether curcumin-induced cell death in malignant breast cancer cells was associated with apoptosis. Both TRAIL (100 ng/ml), a representative apoptotic inducer [20], and curcumin (40 μM) induced similar levels of cytotoxicity in MDA-MB-435S cells. TRAIL also induced the proteolytic processing of caspase-3 and PARP, a substrate of caspase-3 [21], and TRAIL-induced cell death as well as the processing of caspase-3 and PARP was effectively blocked by the pan-caspase inhibitor z-VAD-fmk (Figs. 1B and 1C). By contrast, curcumin-induced cell death was not inhibited by z-VAD-fmk, and curcumin did not induce the processing of caspase-3 or PARP (Figs. 1B and 1C). Moreover, overexpression of Bcl-2, Bcl-xL, survivin or XIAP in MDA-MB-435S cells effectively blocked TRAIL-induced cell death, but not curcumin-induced cell death (Fig. 1D). Similar results were obtained in MDA-MB-231 cells following

treatment with curcumin or TRAIL (Supplementary Fig. S1). Taken together, these results demonstrate that curcumin induces non-apoptotic cell death in these malignant breast cancer cells.

Malignant breast cancer cells (MDA-MB-231, MDA-MB-435S, and Hs578T) treated with curcumin exhibited vacuolation that preceded cell death (Fig. 2A), indicating that curcumin-induced cell death may be associated with autophagy. We have recently shown that sodium selenite induces autophagic cell death in various glioma cells [18]; thus, we first compared the effects of selenite and curcumin on the expression of the autophagy marker LC3 in breast cancer cells. LC3 expression was diffuse in untreated MDA-MB-435S sublines stably expressing GFP-LC3 [17], but was converted to a high-intensity, dot-like expression pattern by treatment with 6 μM selenite (Fig. 2B). However, the GFP-LC3 expression pattern was not altered by treatment with 40 μM curcumin (Fig. 2B). Furthermore, pretreatment with an autophagy inhibitor (such as 3-MA or bafilomycin A) or siRNA-mediated suppression of autophagy-associated ATG genes (such as ATG6 or ATG7) effectively blocked vacuolation and subsequent selenite-induced cell death in MDA-MB-435S cells, but did not affect curcumin-induced vacuolation or cell death (Figs. 2C and 2D). Collectively, these results demonstrate that curcumin does not induce autophagic cell death in malignant breast cancer cells.

Curcumin induces paraptosis accompanied by swelling and fusion of mitochondria or ER in malignant breast cancer cells

Next, we investigated whether the observed curcumin-induced vacuoles originated from mitochondria or the ER, using MBA-MB-435S sublines transfected with the

pEYFP-Mito plasmid to label mitochondria (YFP-Mito cells), or the pEYFP-ER plasmid to label the ER (YFP-ER cells). As shown in Fig. 3A, mitochondria in untreated YFP-Mito cells exhibited an elongated morphology, and the ER in untreated YFP-ER cells appeared as a reticulate structure. Following curcumin treatment for 8 h, numerous vacuoles were clearly discernible by phase-contrast microscopy. Mitochondrial fluorescence in YFP-Mito cells primarily co-localized with vacuoles near the nucleus of a given cell, and ER fluorescence in YFP-ER cells mainly co-localized with vacuoles scattered at the cellular periphery. These observations indicate that curcumin-induced vacuoles originate from both mitochondria and the ER. At 16 h, there were fewer mitochondria- or ER-derived vacuoles, but the existing vacuoles were much larger. Further staining of curcumin-treated YFP-ER cells with MitoTracker-Red revealed that the mitochondria-derived vacuoles were near the nuclei and did not overlap with the ER-derived vacuoles, which were peripheral to the mitochondria-derived vacuoles (Fig. 3B).

Transmission electron microscopy also demonstrated that swelling of both the ER and mitochondria could often be detected within 4 h of curcumin treatment in MDA-MB-435S cells (Fig. 3C). At 8 h, mitochondria were often observed to fuse, leading to the formation of megamitochondria; at 12 h, fusion among swollen portions of the ER was evident and contributed to the dilation of vacuoles. At time points beyond 12 h, rates of fusion of mitochondria and the ER increased until the cells were almost fully occupied by a few large megamitochondria and expanded ER-derived vacuoles. However, autophagosomes or autophagolysosomes were rarely detected. Furthermore, staining of YFP-Mito cells or YFP-ER cells with Lyso-Tracker Red demonstrated that mitochondria- or ER-derived swollen vacuoles did not co-localize with lysosomes (Fig.

3D). Taken together, these results indicate that curcumin-induced vacuoles were the result of the swelling and fusion of mitochondria or ER, rather than a reflection of entrapment of these organelles within autophagosome and subsequent fusion with lysosomes. In contrast to malignant breast cancer cells, normal MCF-10A cells and HMECs treated with 40 μM curcumin for 24 h showed no evidence of cellular vacuolation or cell death (Fig. 3E). Furthermore, staining of these cells with MitoTracker-Green or ER Tracker-Red demonstrated that mitochondrial and ER structures were not altered by treatment with curcumin (Fig. 3E), indicating that curcumin induces dilation of mitochondria and the ER selectively in malignant cancer cells and not in normal breast cells.

Given that mitochondrial and ER enlargement was recently reported to be a characteristic of paraptosis [11,14,15], we next examined whether curcumin-induced cell death in malignant breast cancer cells shared other features of paraptosis. Pretreatment of MDA-MB-435S cells with cycloheximide (CHX) effectively blocked curcumin-induced cell death (Fig. 4A), as well as mitochondrial and ER expansion (Fig. 4B), suggesting that protein synthesis is required for this process. In addition, the levels of AIP-1/Alix protein, a known inhibitor of paraptosis [12,16], were downregulated by curcumin in MDA-MB-231, MDA-MB-435S and Hs578T cells, but not in MCF-10A cells (Fig. 4C and Supplementary Fig. S2). Furthermore, forced overexpression of AIP-1/Alix in MDA-MB-435S or Hs578T cells significantly attenuated curcumin-induced cell death compared with non-transfected or pcDNA3-transfected cells (Fig. 4D and Supplementary Fig. S3).

We next examined the activities of MAP kinases following treatment of MDA-MB-231 and MDA-MB-435S cells with curcumin, and found that p38 activity was not

affected (Fig. 5A). By contrast, the activities of JNKs were significantly increased from 4 h after curcumin treatment (Fig. 5A and Supplementary Fig. S4), and ERKs were transiently activated, peaking at approximately 4 h post-treatment. Interestingly, normal MCF-10A cells treated with curcumin showed no change in ERK or JNK activity, but did show a transient increase in p38 activity. An experiment designed to test the functional significance of MAP kinases in this process showed that curcumin-induced cell death in MDA-MB-435S cells was not affected by inhibition of p38 activity with SB203580, but was significantly decreased by the JNK and MEK inhibitors, SP600125 and U0126, respectively (Fig. 5B). These results indicate that JNKs and ERKs may positively regulate curcumin-induced cell death. We found that JNK inhibition by SP600125 more effectively inhibited curcumin-induced ER dilation than mitochondrial dilation, whereas MEK inhibition by U0126 blocked curcumin-induced dilation of both mitochondria and ER (Fig. 5C). A further examination of the role of ERKs using siRNAs showed that curcumin-induced cell death was significantly inhibited by siRNA-mediated suppression of ERK2 but not ERK1 (Fig. 5D). Collectively, our results demonstrate that the induction of paraptosis may contribute to the selective cytotoxicity of curcumin to malignant breast cancer cells.

Proteasomal dysfunction contributes to curcumin-induced paraptosis

Curcumin was recently shown to inhibit proteasomal function [22,23], so we next examined whether impairment of proteasomal function is also associated with curcumin-induced paraptosis. Western-blot analysis using an anti-ubiquitin antibody demonstrated progressive accumulation of poly-ubiquitinated proteins in curcumin-

treated MDA-MB-231 and MDA-MB-435S cells, but not in MCF-10A cells (Fig. 6A). Immunocytochemistry using an anti-ubiquitin antibody revealed similar results (Supplementary Fig. S5). Proteasome inhibition has been shown to induce the accumulation of misfolded proteins in the ER lumen and impose ER stress [24]. Therefore, we further examined whether proteins associated with ER stress are also differentially modulated by curcumin in cancer versus normal cells. Curcumin treatment significantly increased phosphorylation levels of eIF2α as well as the protein levels of GRP78/94 and CHOP in MDA-MB-435S and MDA-MB-231 cells, but not in MCF-10A cells (Fig. 6A and Supplementary Fig. S6), indicating that proteasomal dysfunction and/or severe ER stress may contribute to the preferential effects of curcumin on malignant breast cancer cells. Thus, we next asked whether proteasomal dysfunction is important for induction of the observed paraptotic changes, including mitochondrial and/or ER dilation. Fluorescence microscopic observation showed that treatment of YFP-Mito cells and YFP-ER with proteasome inhibitors (1 μM MG132, 20 μM lactacystin, or 20 μM ALLN) induced vacuole formation. Interestingly, cellular vacuoles in these cells mainly originated from the ER, whereas mitochondria were fragmented but not dilated (Fig. 6B), indicating that proteasomal dysfunction is mainly responsible for ER-associated events in paraptosis. Next, we examined whether paraptotic changes were also induced by other ER stress inducers. Interestingly, brefeldin A, tunicamycin, and thapsigargin did not induce vacuolation and accumulation of poly-ubiquitinated proteins in the treated cells, although, like curcumin, they did up-regulate GRP78/94 and CHOP (Fig. 6C and Supplementary Fig. S7). In addition, these ER stress inducers stimulated processing of caspase-4, -3 and -7, demonstrating that they induce ER stress-mediated apoptosis. These results indicate that proteasomal

dysfunction, rather than ER stress itself, is more important for the induction of curcumin-induced paraptosis. In addition, proteasome inhibition may be necessary, but not sufficient for curcumin-induced paraptosis, suggesting the presence of the other signals that are responsible for mediating the paraptotic events in mitochondria.

Mitochondrial superoxide triggers curcumin-induced paraptosis

We next tested the possible involvement of reactive oxygen species (ROS) in curcumin-induced paraptosis, based on previous reports that curcumin generates ROS (particularly the superoxide anion) during apoptosis [25]. Flow cytometry analysis using H_2DCF-DA and MitoSOX Red, a fluorescent probe used to detect mitochondrial superoxide [26], demonstrated that ROS levels, in particular mitochondrial superoxide levels, were markedly increased in MDA-MB-435S cells by treatment with 40 μM curcumin, beginning 1 h after exposure (Fig. 7A and Supplementary Fig. S8). Notably, however, the same treatment had no such effect on superoxide or ROS levels in MCF-10A cells. To examine the functional significance of ROS in curcumin-induced cell death, we pretreated MDA-MB-435S cells with various antioxidants and then exposed the cells to 40 μM curcumin for 24 h. Curcumin-induced cytotoxicity was significantly blocked by pretreatment with the general antioxidants, NAC, GSH, or the MnSOD mimetic, MnTBAP in their dose-dependent manner. However interestingly, pretreatment with PEG-catalase did not affect the curcumin-induced cell death at the concentrations that effectively blocked H_2O_2-induced increase in ROS levels and subsequent cell death (Fig.7B and Supplementary Fig. S9). To further confirm the role of MnSOD or catalase in curcumin-induced cell death more clearly, we employed MDA-MB-435S sublines

stably overexpressing MnSOD or catalase. Cell death induced by 40 μM curcumin was also significantly blocked by overexpression of MnSOD, but not catalase (Fig. 7C). In addition, curcumin-induced mitochondrial and ER dilation was almost completely blocked by pretreatment with 5 mM NAC, 5 mM GSH, or 100 μM MnTBAP, but not by 1500 U/ml PEG-catalase (Fig. 7D). Next, we investigated the role of mitochondrial superoxide in curcumin-induced paraptotic signals. We found that MnTBAP pretreatment blocked both curcumin-induced downregulation of Alix, transient activation of ERK, accumulation of poly-ubiquitinated proteins and ER stress responses, including upregulation of GRP78/94 and CHOP (Fig. 8A and Supplementary Fig. S10), indicating that mitochondrial superoxide has a critical role as an initial signal in curcumin-induced paraptosis (Fig. 8B). By contrast, curcumin-induced activation of JNK was not affected by MnTBAP pretreatment, indicating that the involvement of JNK in curcumin-induced paraptosis may be independent of mitochondrial superoxide (Figs. 8A, 8B, and Supplementary Fig. S10).

Taken together, our results demonstrate that both the production of mitochondrial superoxide and proteasomal impairment contribute to curcumin-induced paraptosis in malignant breast cancer cells.

Discussion

Therapeutic selectivity, or preferential killing of malignant cancer cells without significant toxicity to normal cells, is one of the most desirable properties of a potential cancer chemotherapeutic agent. In our study, curcumin demonstrated preferential

cytotoxicity to malignant breast cancer cells over normal breast cells. Consistent with our results, curcumin has demonstrated selective killing of various cancer cell types, while sparing normal cells [3-5]. However, the mechanism underlying the selective cytotoxicity of curcumin against cancer is not yet well understood.

Although caspase-mediated apoptosis is the best-defined cell death program engaged by antitumor agents, studies have shown that apoptosis may not be the major death mode in solid tumors following chemotherapy, and malignant cancer cells tend to resist induction of apoptosis by current treatment protocols [27,28]. Therefore, a better understanding of the regulatory mechanisms governing the different types of non-apoptotic death may aid the development of new and improved strategies for treating malignant cancers. Here, we show for the first time that the paraptosis-inducing activity of curcumin contributes to its selective cytotoxicity against malignant breast cancer cells. Cellular shrinkage, apoptotic bodies, caspase dependency and inhibition of cell death by overexpression of various antiapoptotic proteins, all of which are characteristics of apoptosis, are rarely detected in malignant breast cancer cells treated with curcumin. Although curcumin induced vacuolation that preceded cell death in malignant breast cancer cells, this vacuolation resulted from the swelling and subsequent fusion of the mitochondria or ER, not from autophagy. As a result, cells in the late phase of curcumin treatment contained small numbers of megamitochondria and a substantially expanded ER, consistent with the idea that the irrecoverable functional loss of these organelles led to irreversible cell death. In addition, paraptotic characteristics, such as a requirement for protein synthesis [11], negative involvement of AIP-1/Alix [12,16] and positive involvement of ERK and JNK [12], were commonly observed in curcumin-treated malignant breast cancer cells, but not in normal breast

cells.

In this study, we further attempted to investigate the underlying mechanisms involved in curcumin-induced paraptosis. We found that curcumin-treated malignant breast cancer cells, but not in normal cells, exhibited significant proteasomal dysfunction and ER stress. ER stress can be induced by agents/conditions that interfere with protein glycosylation (such as tunicamycin), protein transport (such as brefeldin A) and calcium imbalance (such as thapsigargin) [29-31]. In addition, inhibition of proteasome activity has been reported to increase the accumulation of ubiquitinated proteins in the ER, leading to ER stress [32]. An investigation of the functional significance of proteasome dysfunction and/or ER stress in paraptotic events showed that treatment of malignant breast cancer cells with well-known proteasome inhibitors (MG132, lactacystin or ALLN) mainly induced the formation of ER-derived vacuoles (Fig. 6B). By contrast, various ER stress inducers, including brefeldin A, tunicamycin and thapsigargin, did not induce the accumulation of poly-ubiquitinated proteins, but instead activated caspase-4, -3, and -7 (Fig. 6C and Supplementary Fig. S7), effects that were not associated with curcumin treatment. These results therefore indicate that proteasome impairment by curcumin contributes to paraptotic changes in the ER, with features distinct from ER stress-induced apoptosis. Therefore, proteasomal dysfunction may be necessary, but not sufficient, for curcumin-induced paraptosis, suggesting the existence of other signals that are responsible for mitochondrial paraptotic changes. The following evidence supports our conclusion that mitochondrial superoxide, rather than H_2O_2, has a critical early role in the curcumin-induced paraptotic changes seen in both mitochondria and the ER; 1) Mitochondrial superoxide levels were rapidly and progressively increased following curcumin treatment (Fig. 7A and Supplementary Fig.

S8). 2) Both curcumin-induced vacuolation of mitochondria and ER and subsequent cell death were almost completely blocked by MnTBAP, but not by PEG-catalase (Figs. 7B and 7D). 3) Overexpression of MnSOD, but not catalase, significantly inhibited curcumin-induced cell death (Fig. 7C). 4) Scavenging of mitochondrial superoxide by pretreatment with MnTBAP inhibited the curcumin-induced paraptotic responses, including Alix downregulation and ERK activation, and also blocked poly-ubiquitinated protein accumulation and ER stress responses (Fig. 8A and Supplementary Fig. S10).

As shown in Fig. 7B and 7D, both NAC and GSH exerted a strong blocking effect on curcumin-induced paraptosis, whereas either PEG-catalase or overexpression of catalase did not (Figs. 7B, 7C and 7D). NAC can act as an antioxidant through at least two different processes: (1) scavenging ROS through a reaction with its thiol group, and (2) stimulating glutathione synthesis after being converted to cysteine and thereby serving as a GSH donor. Therefore, we tested whether NAC and GSH might exert their inhibitory effect on curcumin-induced cell death by modulating GSH levels, rather than by scavenging H_2O_2. When we analyzed the changes in intracellular GSH levels following curcumin treatment, we found that exposure of MDA-MB-435S cells to curcumin induced a rapid time- and dose-dependent reduction of intracellular GSH levels (Supplementary Fig. S11A). Furthermore, curcumin-induced cell death in MDA-MB-435S cells was dose-dependently accelerated by L-buthionine-[S,R]-sulfoximine (BSO), a glutathione synthesis inhibitor, ethacrynic acid (EA), an inhibitor of glutathione S-transferase that catalyzes GSH-substrate conjugation, diethyl maleate (DEM), a thiol depletor, and 1,3-bis(2-chloroethyl)-1-nitrosourea (BCNU), a glutathione reductase inhibitor (Supplementary Fig. S11B). A number of lines of evidence have shown that deficiencies in intracellular GSH impair cellular antioxidant

defenses and result in the accumulation of ROS [33,34]. In our study, pretreatment with NAC and GSH reduced curcumin-induced increase in the mitochondrial superoxide levels, whereas pretreatment with BSO, ethacrynic acid, DEM, or BCNU potentiated it (Supplementary Fig. S11C). Taken together, these results suggest that modulation of intracellular GSH levels may play a key role in curcumin-induced paraptosis, possibly contributing to mitochondrial superoxide production. Curcumin is a Michael acceptor and thus can react with sulfhydryl groups [35]. It has been shown to induce mitochondrial membrane permeability transition pores through membrane protein thiol oxidation [36]. Interestingly, curcumin was reported to form a covalent adduct with the nascent selenol/thiol of the active site of thioredoxin reductase, shifting this enzyme from an antioxidant to a prooxidant [37]. Considering these previous results, we cannot exclude the possibility that thiol oxidation of the protein(s) affecting the cellular redox status may contribute to curcumin-induced paraptosis in malignant breast cancer cells.

Interestingly, inhibition of ERK with U0126 blocked dilation of both mitochondria and the ER (Fig. 5C). Furthermore, ERK inhibition also inhibited the accumulation of poly-ubiquitinated proteins and the ER stress response (Supplementary Fig. S12 and Fig. 8B). Collectively, ERKs (specifically ERK2) may act as a downstream mediator of mitochondrial superoxide in curcumin-induced paraptotic signaling. By contrast, MnTBAP treatment did not affect curcumin-induced JNK activation (Fig. 8A), and JNK inhibition with SP600125 mainly attenuated ER dilation without affecting mitochondrial dilation (Fig. 5C). Furthermore, JNK inhibition partially blocked curcumin-induced accumulation of poly-ubiquitinated proteins and ER stress responses (Supplementary Fig. S12). Previous reports have been shown that ERK signaling cascade is important for the induction of mitochondrial vacuolation [38] and oxidative

stress-induced apoptosis is mediated by ERK1/2 phosphorylation but not by JNK1/2 [39]. These results indicate that JNK may primarily contribute to curcumin-induced ER dilation, although the detailed regulatory mechanisms remain to be determined.

To test whether curcumin-induced paraptosis is restricted to malignant breast cancer cells, we examined the effect of curcumin on other types of cancer cells. We found that curcumin induced cytopalsmic vacuolation cell death in DLD-1 and SW837 colon cancer cells as well as in SNU-387 and SNU-449 hepatoma cells (Supplementary Fig. S13). In particular, the effects of z-VAD-fmk, cycloheximide, antioxidants, and the inhibitors of MAP kinases on curcumin-induced cell death in DLD-1 and SW837 cells were very similar to those observed in malignant breast cancer cells, demonstrating that curcumin induces paraptosis also in these cells (Supplementary Fig. S14). Contrastingly, curcumin induced mixed modes of cell death, including apoptosis, necrosis and paraptosis, in HCT116, SW480 colon cancer cells, HepG2 and SK-Hep-1 hepatoma cells. The underlying mechanisms by which curcumin induces different modes of cell death depending on the cell type remain to be clarified. Epidemiological studies [40] have provided evidence that the low incidence of colorectal cancer observed in India is associated with diets high in curcumin. Curcumin exhibits great promise as a therapeutic agent and is currently in human clinical trials for colon and pancreatic cancer and multiple myeloma [41]. Notably, however, a recent study has shown that curcumin may exert tumor-promoting activity in the lung, possibly by producing a pro-oxidant environment [42]. These results suggest that the clinical use of curcumin as an anti-cancer agent may require extensive preclinical studies to consider potential organ-specific effects of curcumin.

In conclusion, induction of paraptosis may contribute to curcumin-induced

cytotoxicity in malignant breast cancer cells that exhibit apoptotic machinery defects. Thus, investigation of the molecular basis of curcumin-induced paraptosis may provide potential new therapeutic strategies for selectively killing malignant breast cancer cells through induction of paraptosis.

Acknowledgement

We thank Dr. Yoshimori of Osaka University, Japan, for GFP-LC3 construct. This work was supported by the grant of the Korea Healthcare technology R&D Project, Ministry of Health & Welfare, Republic of Korea (A080426).

References

[1] Ammon, H. P.; Wahl, M. A. Pharmacology of Curcuma longa. *Planta Med.* **57:**1-7; 1991.

[2] Shishodia, S.; Chaturvedi, M. M.; Aggarwal, B. B. Role of curcumin in cancer therapy. *Curr. Probl. Cancer.* **31:**243-305; 2007.

[3] López-Lázaro, M. Anticancer and carcinogenic properties of curcumin: considerations for its clinical development as a cancer chemopreventive and chemotherapeutic agent. *Mol. Nutr. Food Res.* **52:**S103-127; 2008.

[4] Shankar, S.; Srivastava, R. K. Involvement of Bcl-2 family members, phosphatidylinositol 3'-kinase/AKT and mitochondrial p53 in curcumin

(diferulolylmethane)-induced apoptosis in prostate cancer. *Int. J. Oncol.* **30:**905-918; 2007.

[5] Syng-Ai, C.; Kumari, A. L.; Khar, A. Effect of curcumin on normal and tumor cells: role of glutathione and bcl-2. *Mol. Cancer Ther.* **3:**1101-1108; 2004.

[6] Karunagaran, D.; Rashmi, R.; Kumar, T. R. Induction of apoptosis by curcumin and its implication for cancer therapy. *Curr. Cancer Drug Targets*. **5:**117-129; 2005.

[7] Reuter, S.; Eifes, S.; Dicato, M.; Aggarwal, B. B.; Diederich, M. Modulation of anti-apoptotic and survival pathways by curcumin as a strategy to induce apoptosis in cancer cells. *Biochem. Pharmacol*. **76:**1340-1351; 2008.

[8] Wolanin, K.; Magalska, A.; Mosieniak, G.; Klinger, R.; McKenna, S.; Vejda, S.; Sikora, E.; Piwocka, K. Curcumin affects components of the chromosomal passenger complex and induces mitotic catastrophe in apoptosis-resistant Bcr-Abl-expressing cells. *Mol. Cancer Res.* **4:**457-469; 2006.

[9] Magalska, A.; Sliwinska, M.; Szczepanowska, J.; Salvioli, S.; Franceschi, C.; Sikora, E. Resistance to apoptosis of HCW-2 cells can be overcome by curcumin- or vincristine-induced mitotic catastrophe. *Int. J. Cancer.* **119:**1811-1818; 2006.

[10] Aoki, H.; Takada, Y.; Kondo, S.; Sawaya, R.; Aggarwal, B. B; Kondo, Y. Evidence that curcumin suppresses the growth of malignant gliomas in vitro and in vivo through induction of autophagy: role of Akt and extracellular signal-regulated kinase signaling pathways. *Mol. Pharmacol*. **72:**29-39; 2007.

[11] Sperandio, S.; de Belle, I.; Bredesen, D. E. An alternative, nonapoptotic form of programmed cell death. *Proc. Natl. Acad. Sci. U S A* **97:**14376-14381; 2000.

[12] Sperandio, S.; Poksay, K.; de Belle, I.; Lafuente, M. J.; Liu, B.; Nasir, J.;

Bredesen, D. E. Paraptosis: mediation by MAP kinases and inhibition by AIP-1/Alix. *Cell Death Differ.* **11:**1066-1075; 2004.

[13] Fombonne, J.; Padrón, L.; Enjalbert, A.; Krantic, S; Torriglia, A. A novel paraptosis pathway involving LEI/L-DNaseII for EGF-induced cell death in somato-lactotrope pituitary cells. *Apoptosis* **11:**367-375; 2006.

[14] Wang, Y.; Li, X.; Wang, L.; Ding, P.; Zhang, Y.; Han, W.; Ma, D. An alternative form of paraptosis-like cell death, triggered by TAJ/TROY and enhanced by PDCD5 overexpression. *J. Cell Sci*. **117:**1525-1532; 2004.

[15] Hoa, N. T.; Zhang, J. G.; Delgado, C. L.; Myers, M. P.; Callahan, L. L.; Vandeusen, G.; Schiltz, P. M.; Wepsic, H. T.; Jadus, M.R. Human monocytes kill M-CSF-expressing glioma cells by BK channel activation. *Lab Invest.* **87:**115-129; 2007.

[16] Valamanesh, F.; Torriglia, A.; Savoldelli, M.; Gandolphe, C.; Jeanny, J. C.; BenEzra, D.; Behar-Cohen, F. Glucocorticoids induce retinal toxicity through mechanisms mainly associated with paraptosis. *Mol. Vis.* **13:**1746-1757; 2007.

[17] Kabeya, Y.; Mizushima, N.; Ueno, T.; Yamamoto, A.; Kirisako, T.; Noda, T.; Kominami, E.; Ohsumi, Y.; Yoshimori, T. LC3, a mammalian homologue of yeast Apg8p, is localized in autophagosome membranes after processing. *EMBO J.* **19:**5720-5728; 2000.

[18] Kim, E. H.; Sohn, S.; Kwon, H. J.; Kim, S. U.; Kim, M. J.; Lee, S. J.; Choi, K. S. Sodium selenite induces superoxide-mediated mitochondrial damage and subsequent autophagic cell death in malignant glioma cells. *Cancer Res.* **67:**6314-6324; 2007.

[19] Ory, D. S.; Neugeboren, B. A.; Mulligan, R. C. A stable human-derived

packaging cell line for production of high titer retrovirus/vesicular stomatitis virus G pseudotypes. *Proc. Natl. Acad. Sci. U S A* **93:**11400-11406; 1996.

[20] Wiley, S. R.; Schooley, K.; Smolak, P. J.; Din, W. S.; Huang, C. P.; Nicholl, J. K.; Sutherland, G. R.; Smith, T. D.; Rauch, C.; Smith, C. A.; et al. Identification and characterization of a new member of the TNF family that induces apoptosis. *Immunity* **3:**673-682; 1995.

[21] Tewari, M.; Quan, L. T.; O'Rourke, K.; Desnoyers, S.; Zeng, Z.; Beidler, D. R.; Poirier, G. G.; Salvesen, G. S.; Dixit, V. M. Yama/CPP32 beta, a mammalian homolog of CED-3, is a CrmA-inhibitable protease that cleaves the death substrate poly (ADP-ribose) polymerase. *Cell* **81:**801-809; 1995.

[22] Jana, N. R.; Dikshit, P.; Goswami, A.; Nukina, N. Inhibition of proteasomal function by curcumin induces apoptosis through mitochondrial pathway. *J. Biol. Chem.* **279:**11680-11685; 2004.

[23] Milacic, V.; Banerjee, S.; Landis-Piwowar, K. R.; Sarkar, F. H.; Majumdar, A. P.; Dou, Q. P. Curcumin inhibits the proteasome activity in human colon cancer cells in vitro and in vivo. *Cancer Res.* **68:**7283-7292; 2008.

[24] Nawrocki, S. T.; Carew, J. S.; Dunner, K. Jr.; Boise, L. H.; Chiao, P. J.; Huang, P.; Abbruzzese, J. L.; McConkey, D. J. Bortezomib inhibits PKR-like endoplasmic reticulum (ER) kinase and induces apoptosis via ER stress in human pancreatic cancer cells. *Cancer Res.* **65:**11510-11519; 2005.

[25] Cao, J.; Liu, Y.; Jia, L.; Zhou, H. M.; Kong, Y.; Yang, G.; Jiang, L. P.; Li, Q. J.; Zhong, L. F. Curcumin induces apoptosis through mitochondrial hyperpolarization and mtDNA damage in human hepatoma G2 cells. *Free Radic. Biol. Med.* **43:**968-975; 2007.

[26] Robinson, K. M.; Janes, M. S.; Pehar, M.; Monette, J. S.; Ross, M. F.; Hagen, T. M.; Murphy, M. P.; Beckman, J. S. Selective fluorescent imaging of superoxide in vivo using ethidium-based probes. *Proc. Natl. Acad. Sci. U S A* **103:**15038-15043; 2006.

[27] Jäättelä, M. Escaping cell death: survival proteins in cancer. *Exp. Cell Res.* **248:**30-43; 1999.

[28] Mathiasen, I. S.; Jäättelä, M. Triggering caspase-independent cell death to combat cancer. *Trends Mol. Med.* **8:**212-220; 2002.

[29] McDowell, W.; Schwarz, R. T. Dissecting glycoprotein biosynthesis by the use of specific inhibitors. *Biochimie.* **70:**1535-1549; 1988.

[30] Misumi, Y.; Misumi, Y.; Miki, K.; Takatsuki, A.; Tamura, G.; Ikehara, Y. Novel blockade by brefeldin A of intracellular transport of secretory proteins in cultured rat hepatocytes. *J. Biol. Chem.* **261:**11398-11403; 1986.

[31] Inesi, G.; Sagara, Y. Thapsigargin, a high affinity and global inhibitor of intracellular Ca^{2+} transport ATPases. *Arch. Biochem. Biophys.* **298:**313-317; 1992.

[32] Mimnaugh, E. G.; Xu, W.; Vos, M.; Yuan, X.; Neckers, L. Endoplasmic reticulum vacuolization and valosin-containing protein relocalization result from simultaneous hsp90 inhibition by geldamamycin and proteasome inhibition by velcade. *Mol. Cancer Res.* **4:**667-681; 2006.

[33] Armstrong, J. S.; Jones, D.P. Glutathione depletion enforces the mitochondrial permeability transition and causes cell death in Bcl-2 overexpressing HL60 cells. *FASEB J.* **16:**1263-1265; 2002.

[34] Stanislawski, L.; Lefeuvre, M.; Bourd. K.; Soheili-Majd, E.; Goldberg, M.;

Périanin, A. TEGMDA-induced toxicity in human fibroblasts is associated with early and drastic glutathione depletion with subsequent production of oxygen reactive species. *J. Biomed. Mater. Res.* **66:**476-482; 2003.

[35] Dinkova-Kostova, A. T.; Massiah, M.A.; Bozak, R. E.; Hicks, R. J.; Talalay, P. Potency of Michael reaction acceptors as inducers of enzymes that protect against carcinogenesis depends on their reactivity with sulfhydryl groups. *Proc. Natl. Acad. Sci. USA*. **98:**3404-3409; 2001.

[36] Morin, D.; Barthelemy, S.; Zini, R.; Labidalle, S.; Tillement, J. P. Curcumin induces the mitochondrial permeability transition pore mediated by membrane thiol oxidation. *FEBS Lett*. **495:**131-136; 2001.

[37] Fang, J.; Lu, J.; Holmgren, A. Thioredoxin reductase is irreversibly modified by curcumin: a novel molecular mechanism for its anticancer activity. *J. Biol. Chem.* **280:**25284-25290; 2005.

[38] Isobe, I.; Maeno, Y.; Nagao, M.; Iwasa, M.; Koyama, H.; Seko-Nakamura, Y.; Monma-Ohtaki, J. Cytoplasmic vacuolation in cultured rat astrocytes induced by an organophosphorus agent requires extracellular signal-regulated kinase activation. *Toxicol. Appl. Pharmacol.* **193:**383-392; 2003.

[39] Lee, Y. J.; Cho, H. N.; Soh, J. W.; Jhon, G. J.; Cho, C. K.; Chung, H. Y.; Bae, S.; Lee, S. J.; Lee, Y. S. Oxidative stress-induced apoptosis is mediated by ERK1/2 phosphorylation. *Exp. Cell Res.* **291:**251-266; 2003.

[40] Sinha, R.; Anderson, D. E.; McDonald, S. S.; Greenwald, P. Cancer risk and diet in India. *J. Postagrad. Med*. **49:**222-228; 2003.

[41] Hatcher, H.; Planalp, R.; Cho, J.; Torti, F. M.; Torti, S. V. Curcumin: from ancient medicine to current clinical trials. *Cell. Mol. Life Sci*. **65:**1631-1652; 2008.

[42] Dance-Barnes, S. T.; Kock, N. D.; Moore, J. E.; Lin, E. Y.; Mosley, L. J.; D'Agostino, R. B.; McCoy, T. P.; Townsend, A. J.; Miller, M. S. Lung tumor promotion by curcumin. *Carcinogensis* **30:**1016-1023; 2009.

Figure legends

Fig. 1. Curcumin induces non-apoptotic cell death in malignant breast cancer cells. (A) Cells were treated with the indicated concentrations of curcumin for 36 h and then viability was assessed using calcein-AM and EthD-1. (B) MDA-MB-435S cells were untreated or pretreated with 25 μM z-VAD-fmk and further treated with 40 μM curcumin or 100 ng/ml TRAIL for the indicated time points. Cellular viability was assessed using calcein-AM and EthD-1. (C) Western blotting of caspase-3, PARP and β-actin. (D) MDA-MB-435S cells were transfected with empty vector (control), Flag-tagged Bcl-2, Bcl-xL, survivin or XIAP and their respective overexpression was confirmed by Western blotting using anti-Flag antibody or the respective antibodies. Respectively transfected cell were treated with 40 μM curcumin or 100 ng/ml TRAIL for the indicated time points. Cellular viabilities were assessed using calcein-AM and EthD-1.

Fig. 2. Curcumin-induced cell death in malignant breast cancer cells is not associated with autophagy. (A) Malignant breast cancer cells were treated with 40 μM curcumin for 12 h and observed. Bars, 20 μm. (B) GFP-LC3 expressing MDA-MB-435S cells were treated with 40 μM curcumin or 6 μM selenite for 8 h, and observed under the fluorescence microscope. Bars, 20 μm. (C) MDA-MB-435S cells were pretreated with 3-methyl adenine (3-MA) or bafilomycin A (Bafilo.) and further treated with 40 μM curcumin or 6 μM selenite for 24 h. Cellular viability was assessed using calcein-AM and EthD-1. Representative images of cells are shown. (D) MDA-MB-435S cells were transfected with 40 nM scrambled negative control RNA, ATG6 siRNA, or ATG7

siRNA and incubated for 24 h. The expressions of ATG6 and ATG7 were analyzed by Western blotting. Transfected cells were treated with 40 μM curcumin or 6 μM selenite for 24 h and cellular viabilities were analyzed using calcein-AM and EthD-1. Representative images of cells are shown. Bars, 20 μm.

Fig. 3. Curcumin-induced vacuoles are originated from both mitochondria and ER. (A) YFP-Mito or YFP-ER cells treated with 40 μM curcumin were observed under a phase contrast and fluorescence microscope. Bars, 20 μm. (B) YFP-ER cells were treated with 40 μM curcumin, further incubated with MitoTracker-Red, and observed. Bars, 20 μm. (C) MDA-MB-435S cells were treated with 40 μM curcumin and transmission electron microscopy was done. Swelling and fusion of mitochondria (*black arrow heads*) or ER (*black arrows*) was progressed following curcumin treatment. Bars, 2 μm. White arrows denote megamitochondria, which are derived from swelling and fusion among mitochondria. (D) YFP-Mito or YFP-ER cells were treated with 40 μM curcumin for the indicated time points, further incubated with LysoTracker-Red, and observed. Bars, 20 μm. (E) MCF-10A cells or HMEC were treated with 40 μM curcumin for 24 h, further incubated with MitoTracker-Green or ER Tracker-Red, and observed under a fluorescence microscope. Bars, 20 μm.

Fig. 4. Curcumin induces paraptosis in malignant breast cancer cells. (A) MDA-MB-435S cells were pretreated with cycloheximide (CHX) and further treated with 40 μM curcumin. Cellular viabilities were assessed using calcein-AM and EthD-1. (B) YFP-Mito or YFP-ER cells were pretreated with 2 μM CHX, further treated with 40 μM curcumin for 24 h, and observed. Bars, 20 μm. (C) Alix is downregulated in malignant

breast cancer cells, but not in MCF-10A cells treated with crucumin. Western blotting of Alix and β-actin in cells treated with 40 μM curcumin. (D) Overexpression of Alix inhibits curcumin-induced cell death. MDA-MB-435S or Hs578T cells were transfected with pcDNA3 or the expression vector encoding Flag-tagged Alix and further treated with 40 μM curcumin for 24 h. Expression of Flag-tagged Alix and β-actin was analyzed by Western blotting. Cellular viabilities were assessed using calcein-AM and EthD-1.

Fig. 5. Role of ERK in curcumin-induced paraptosis. (A) Western blotting of MAP kinases in cells treated with 40 μM curcumin. (B) Effects of the inhibition of MAPK kinases on curcumin-induced cell death. MDA-MB-435S cells were pretreated with SB203580, SP600125, U0126 for 30 min and further treated with 40 μM curcumin for 24 h. (C) Effects of the specific inhibitors of MAP kinase pathways on curcumin-induced dilation of mitochondria and ER. YFP-Mito and YFP-ER cells were pretreated with 20 μM SB203580, 30 μM SP600125, or 20 μM U0126 and further treated with 40 μM curcumin for 16 h. Treated cells were observed under the fluorescence and phase contrast microscope. Bars, 20 μm. (D) MDA-MB-435S cells were transfected with 40 nM control RNA, ERK1 siRNA or ERK2 siRNA, and then treated with 40 μM curcumin for 24 h. Suppression of ERK1 or ERK2 expression by its siRNA transfection was confirmed by Western blotting. Cellular viability was assessed using calcein-AM and EthD-1.

Fig. 6. Proteasomal dysfunction contributes to curcumin-induced ER dilation in malignant breast cancer cells. (A) Western blotting of the expressions of poly-

ubiquitinated proteins, ER stress maker proteins, and β-actin in the cells treated with 40 μM curcumin. (B) YFP-Mito or YFP-ER cells were treated with 1 μM MG132, 20 μM lactacystin, and 20 μM ALLN for 16 h, and 40 μM curcumin for 24 h and then observed. Bars, 20 μm. (C) MDA-MB-435S cells were treated with 40 μM curcumin, and 2 μg/ml brefeldin A, 10 μM tunicamycin, and 4 μM thapsigargin for 36 h and observed. (D) Cells extracts were prepared from MDA-MB-435S cells treated with ER stress inducers for Western blotting.

Fig. 7. Mitochondrial superoxide plays a critical role in curcumin-induced paraptosis. (A) MDA-MB-435S and MCF-10A cells were treated with 40 μM curcumin for 4 h, loaded with H_2DCF-DA or MitoSOX Red, and then total ROS or mitochondrial superoxide levels were respectively analyzed by flow cytometry. (B) Effect of various antioxidants on curcumin-induced cell death. MDA-MB-435S cells were pretreated with various antioxidants at the indicated concentrations for 30 min and further treated with 40 μM curcumin for 24 h. Cellular viabilities were assessed using calcein-AM and EthD-1. (C) Effect of overexpression of MnSOD or Catalase. Cells were treated with 40 μM curcumin for 24 h and cellular viabilities were assessed using calcein-AM and EthD-1. (D) YFP-Mito or YFP-ER cells were pretreated with the indicated antioxidant (5 mM NAC, 5 mM GSH, 100 μM MnTBAP, 1500 U/ml PEG-catalase), further treated with 40 μM curcumin for 16 h, and observed. Bars, 20 μm.

Fig. 8. Mitochondrial superoxide has a critical role as an initial signal in curcumin-induced paraptosis. (A) MDA-MB-435S cells were pretreated with 100 μM MnTBAP, further treated with 40 μM curcumin, and cells extracts were prepared for Western

blotting. (B) Proposed schematic diagram of curcumin-induced paraptotic pathway. Curcumin-induced increase in superoxide levels activates ERK2, leading to mitochondrial swelling and proteasome dysfunction-mediated ER swelling. JNK is also involved in curcumin-induced paraptosis, primarily contributing to ER swelling. Disruption of the structures and irrecoverable functional loss in mitochondria and ER finally lead to irreversible cell death.

Yoon, M. J. et al. Fig. 1.

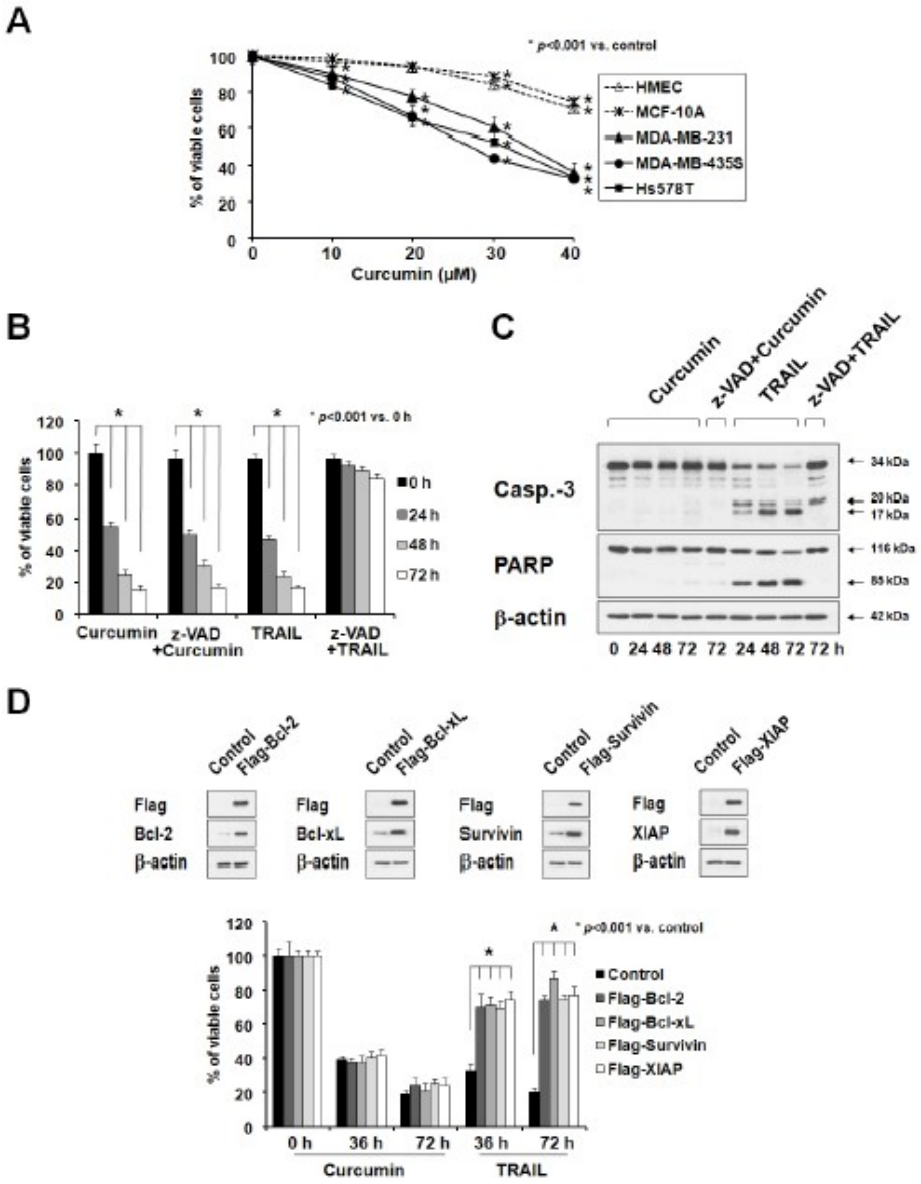

Yoon, M. J. et al. Fig. 2.

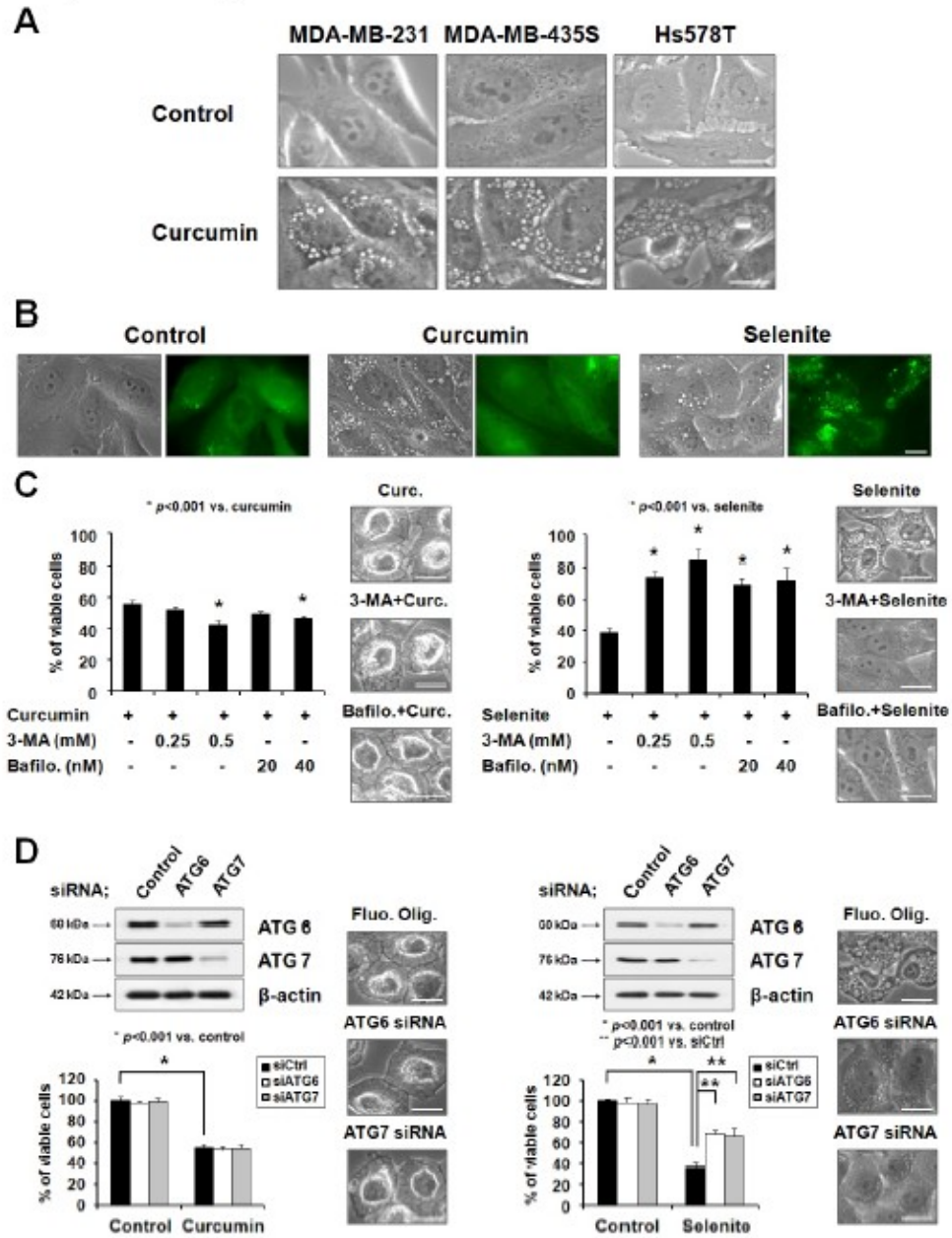

Yoon, M. J. et al. Fig. 3.

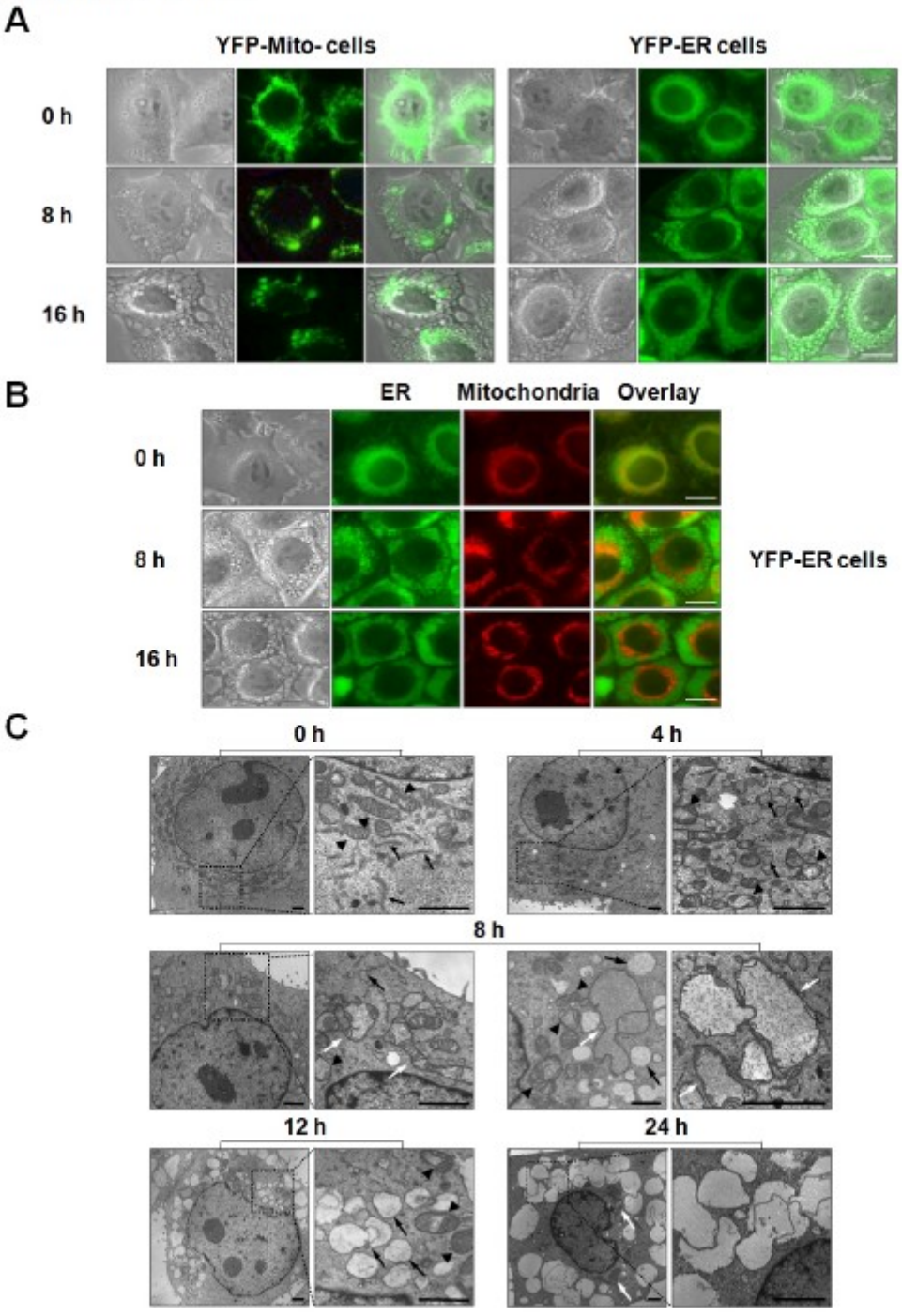

Yoon, M. J. et al. Fig. 3.

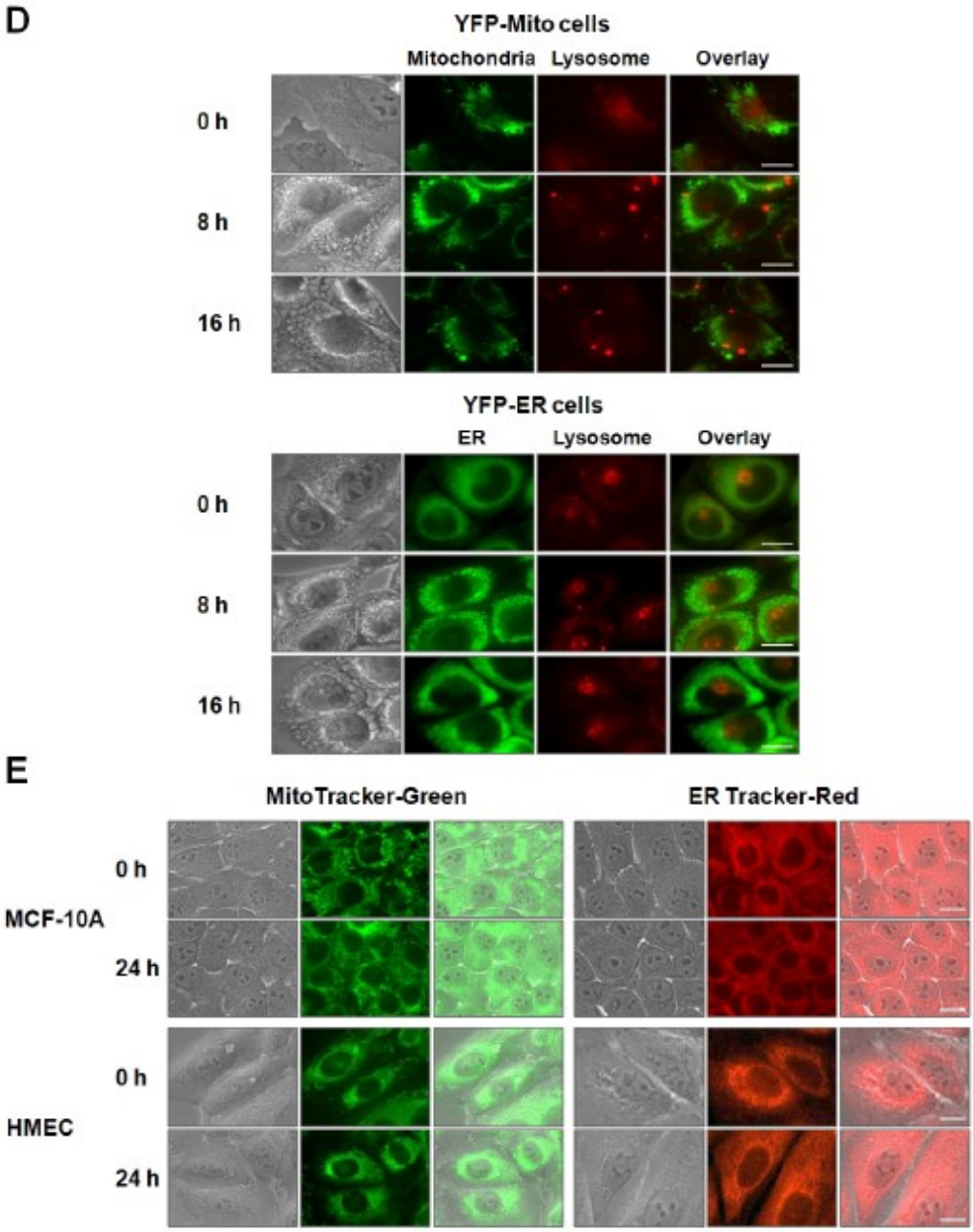

Yoon, M. J. et al. Fig. 4.

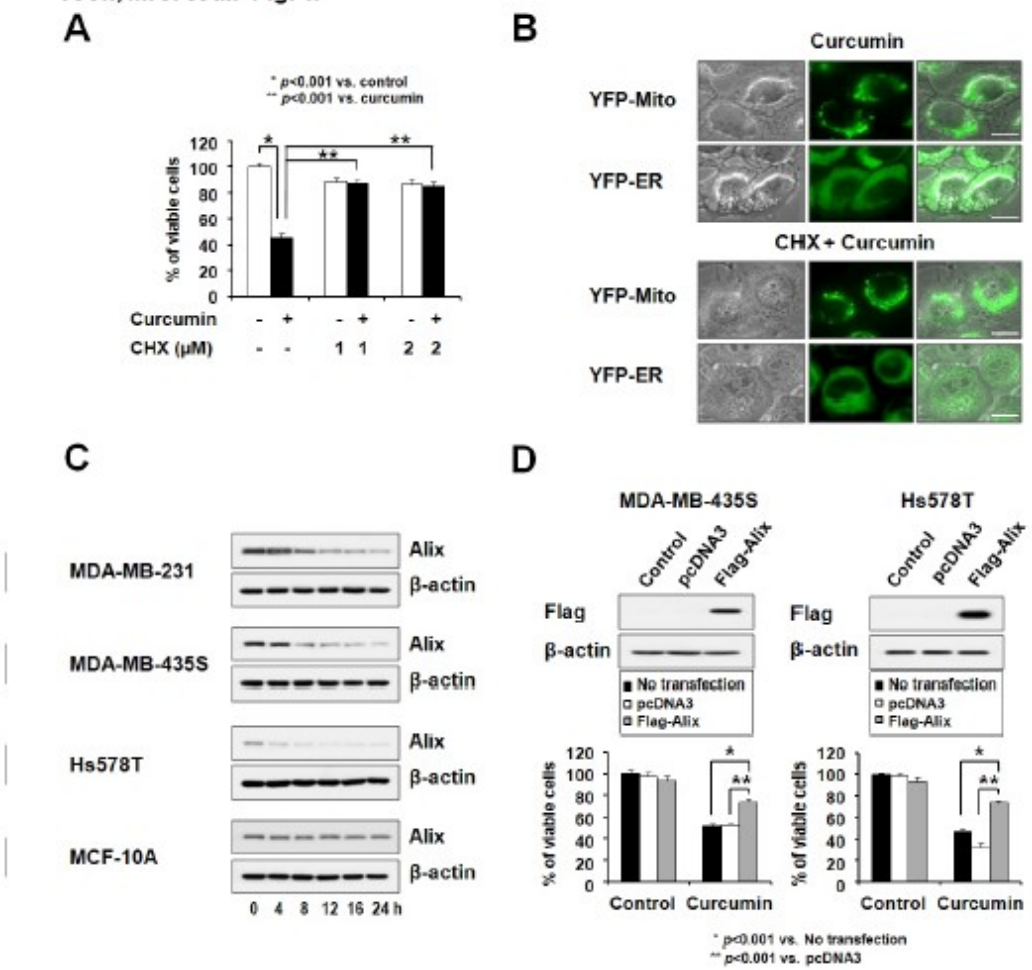

Yoon, M. J. et al. Fig. 5.

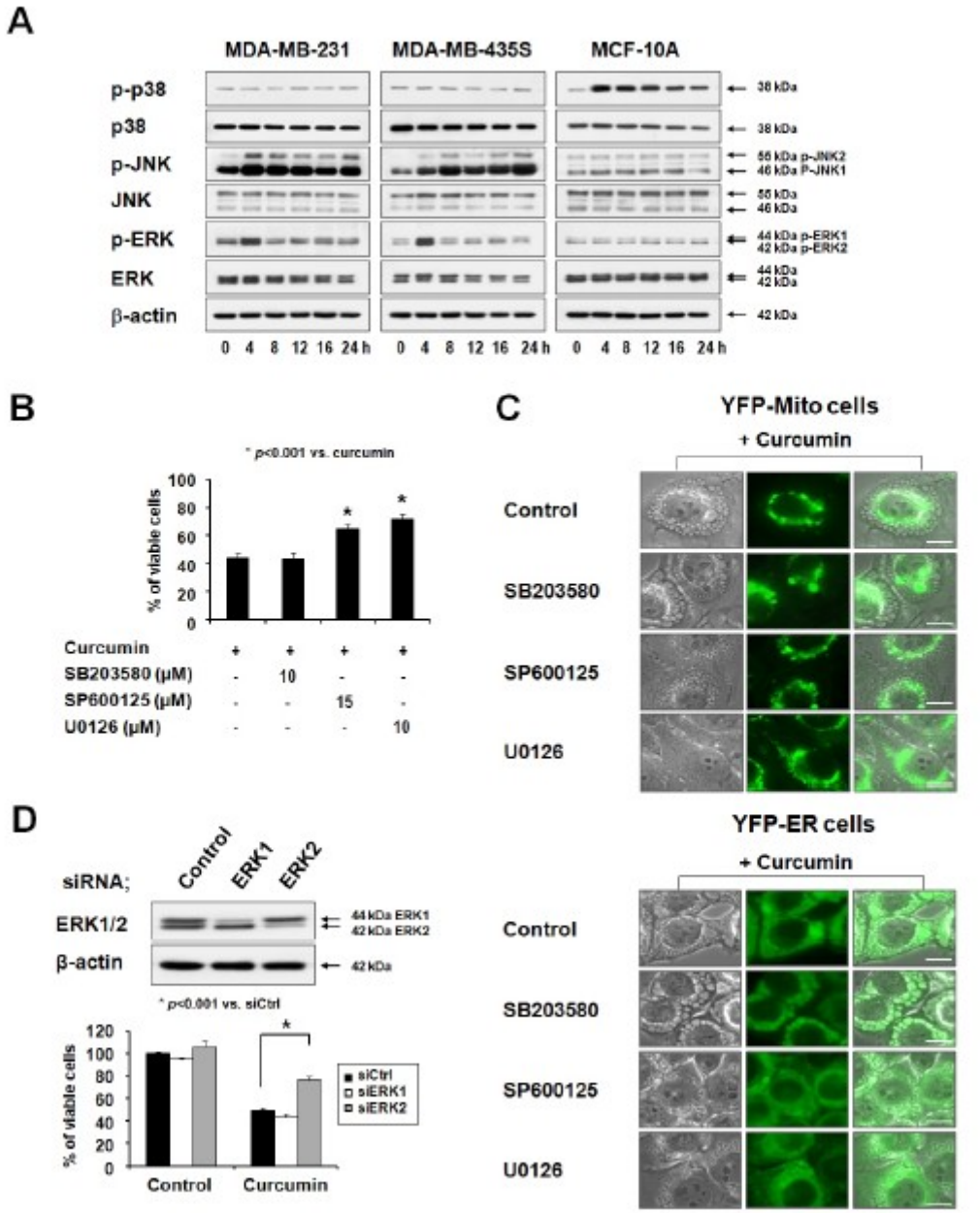

Yoon, M. J. et al. Fig. 6.

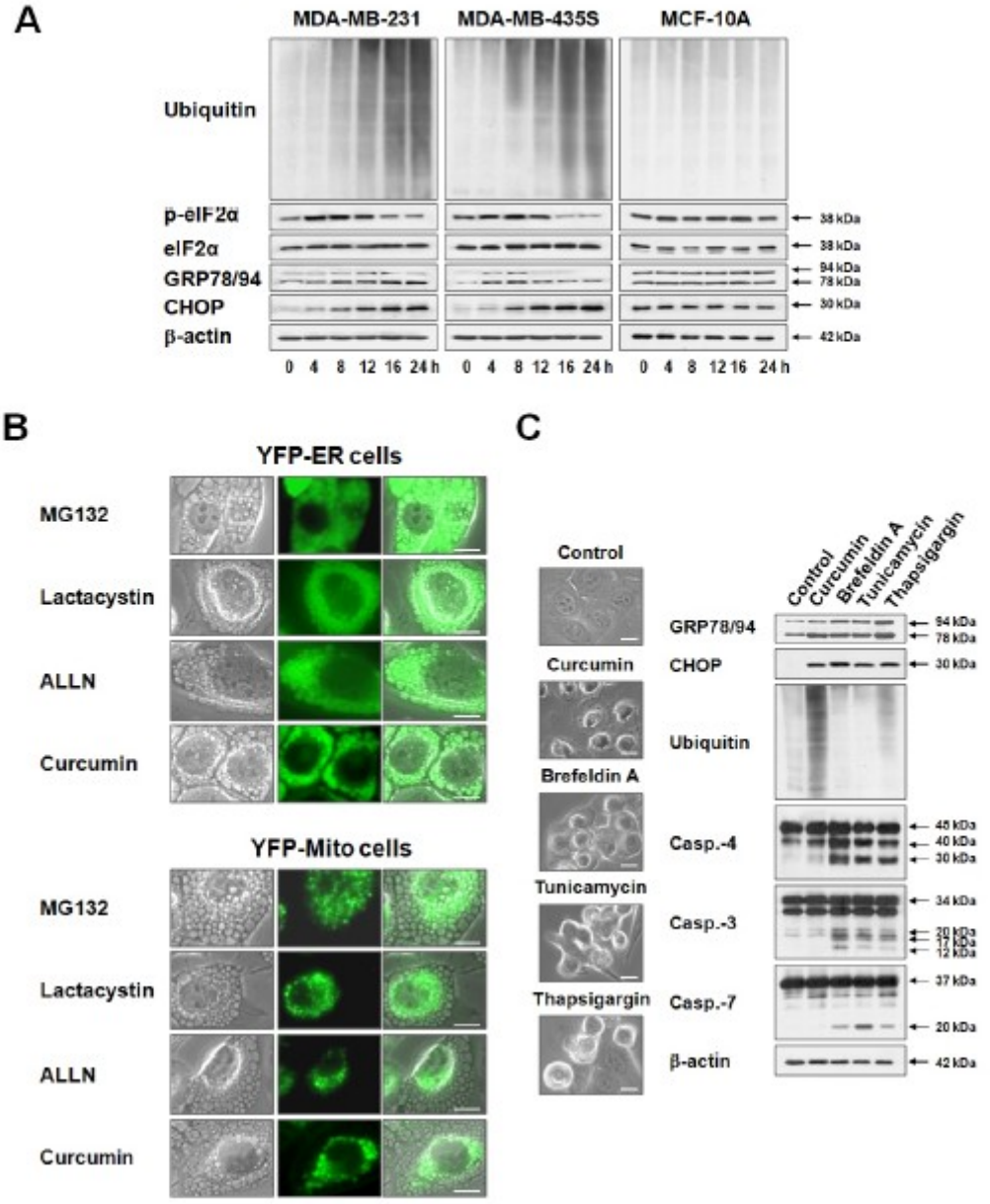

Yoon, M. J. et al. Fig. 7.

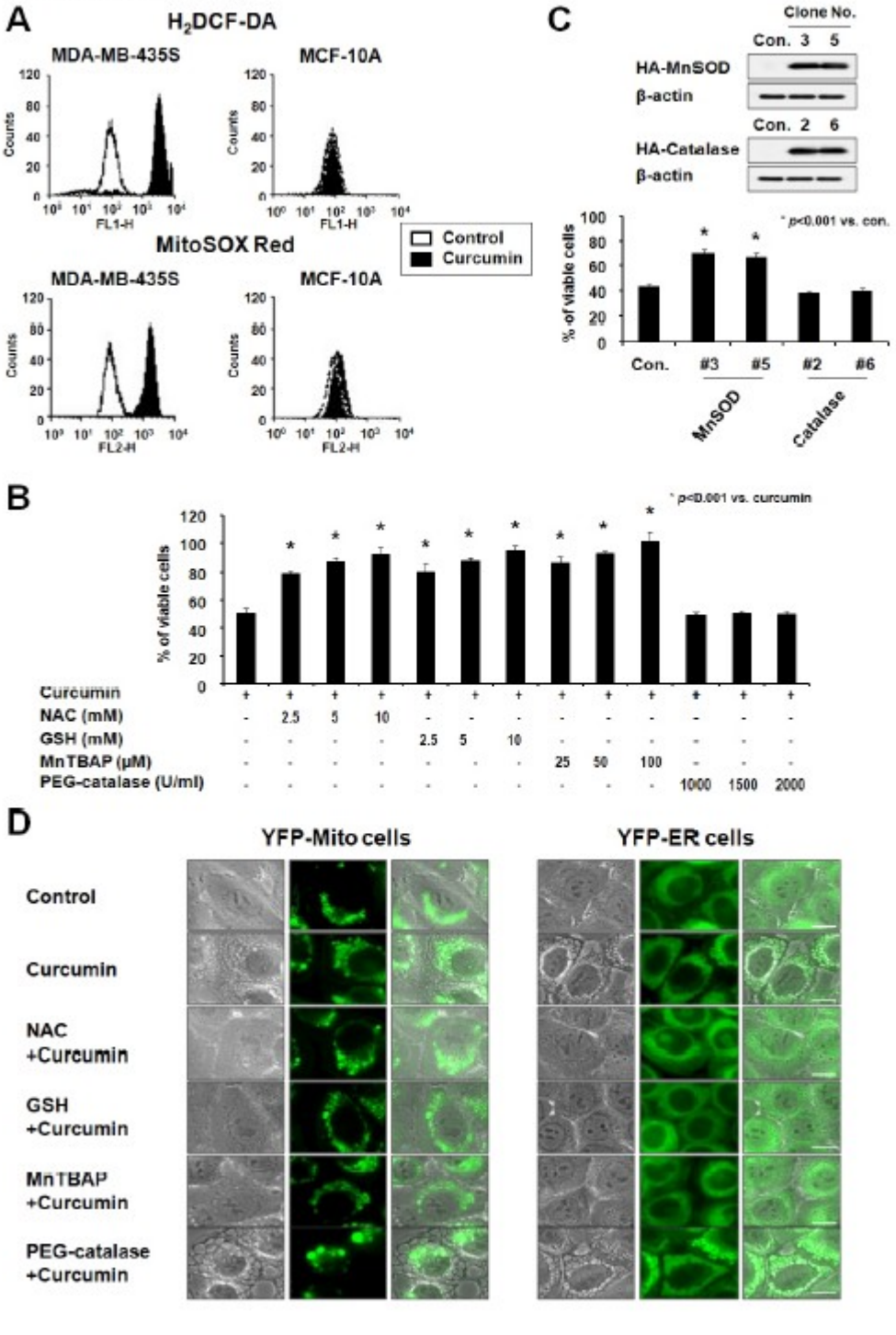

Yoon, M. J. et al. Fig. 8.